Exploiting Weak Noncovalent Cation···π Interaction for Designing a Molecular Container for Storage of Methane Molecules with Lithiated Carbene Superbases

ARTICLE *in* THE JOURNAL OF PHYSICAL CHEMISTRY C · MARCH 2014

Impact Factor: 4.77 · DOI: 10.1021/jp5003319

2 AUTHORS:

Rabindranath Lo

Academy of Sciences of the Czech Republic

27 PUBLICATIONS **126** CITATIONS

SEE PROFILE

Bishwajit Ganguly

Central Salt and Marine Chemicals Research I…

183 PUBLICATIONS **2,246** CITATIONS

SEE PROFILE

THE JOURNAL OF PHYSICAL CHEMISTRY C

Article

pubs.acs.org/JPCC

Exploiting Weak Noncovalent Cation···π Interaction for Designing a Molecular Container for Storage of Methane Molecules with Lithiated Carbene Superbases

Rabindranath Lo and Bishwajit Ganguly*

Computation and Simulation Unit (Analytical Discipline and Centralized Instrument Facility), CSIR—Central Salt & Marine Chemicals Research Institute, Bhavnagar, Gujarat 364 002, India

Supporting Information

ABSTRACT: This study reports the multiprotonation sites exploiting noncovalent interactions to achieve hyperbasicity of an uncharged organic base. A new class of carbene based organic superbase has been designed to attain the proton affinity (PA) value of 301.9 kcal/mol at M06-2X/6-311+G**//B3LYP/6-31+G* level of theory. These designed scaffold molecules can possess three independent protonation sites, which is not available in the literature to date. The stabilization of the protonated forms of the superbases by noncovalent interactions such as C−H$^+$···π interaction is responsible for augmenting the basicity of such carbene systems. The DFT calculated results show that such carbene systems can be suitable candidate for tris-protonation with pK_a(MeCN) value of 43.3 and proton affinity value (MeCN) of 312.1 kcal/mol. Molecular electrostatic potential (MESP) analysis shows the existence of electron density at the reactive sites and the role of substituents to enhance the electron density in such designed systems. There is a good correlation with the absolute minima of the MESP (V_{min}) located for such carbene systems with their calculated proton affinity values. The frontier molecular orbital energy of such carbenes also shows a good relationship with their proton affinity results. These carbene systems can be utilized further for selective binding of lithium ions over sodium ions. Such lithiated organic superbases can be used as a molecular container for the storage of hydrogen and methane molecules. The energy decomposition analysis (EDA) has been performed to explain the role of various factors which contribute to the total binding strength of the hydrogen or methane molecules with lithiated carbene superbases. The localized molecular orbital energy decomposition analysis reveals that the electrostatic and polarization effects are the major contributing factors in interactions with methane and hydrogen molecules. This is the first report where the organic superbase has been exploited as efficient methane storage materials.

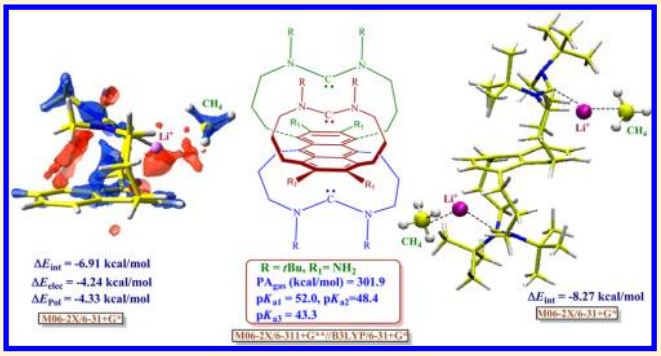

1. INTRODUCTION

Neutral organic superbases are important auxiliary ingredients in modern organic chemistry.[1−3] They involve mild reaction conditions, efficient solubility in most organic solvents, and excellent environment friendly recycling possibilities.[4−6] Several families of compounds such as guanidines, phosphazenes, quinoimines, and Verkade phosphatrane have been reported to exhibit superbasicity in the field of current organic chemistry.[7−32] To improve the basicity of the systems, an increasing number of functional groups are included in the uncharged organic superbases. Several organic superbases are often used as an efficient agent for CO_2 capture process and H_2 storage.[21,33−39] Strong organic bases such as diazabicyclo[5.4.0]-undec-7-ene (DBU), 1,5,7-triazabicyclo[4.4.0]-dec-5-ene (TBD), 1,5-diazabicyclo[4.3.0]-non-5-ene (DBN), and polycyclic diazatricyclo[5.3.1.1^{2,6}]dodecane in conjunction with alcohol were able to capture CO_2 for the formation of the corresponding amidinium/guanidinium alkyl carbonate salts.[19,37] Besides possessing such important properties, the organic superbases often have limitations, such as high toxicity, high price, low functional group capability, low stability, and accessibility only through multistep processes.[3] Thus, the design and synthesis of novel, efficient neutral organic superbases is an important area of research for more than three decades. It is still a challenging topic in the field of organic chemistry due to the distinctive features of neutral organic superbases.

Herein, we have described a series of carbene superbases by achieving super basicity through the interaction of divalent carbon(II) compounds. We have explored the possibility of multiprotonation sites in a single organic base molecule. The synthetically attractive carbene based novel organic superbases can be designed by taking the advantage of noncovalent C−H$^+$···π interactions.[17] Such noncovalent interaction is respon-

Received: January 11, 2014
Revised: March 7, 2014
Published: March 12, 2014

   dx.doi.org/10.1021/jp5003319 | J. Phys. Chem. C 2014, 118, 6680−6689

Scheme 1. Chemical Structures of Designed Organic Superbases

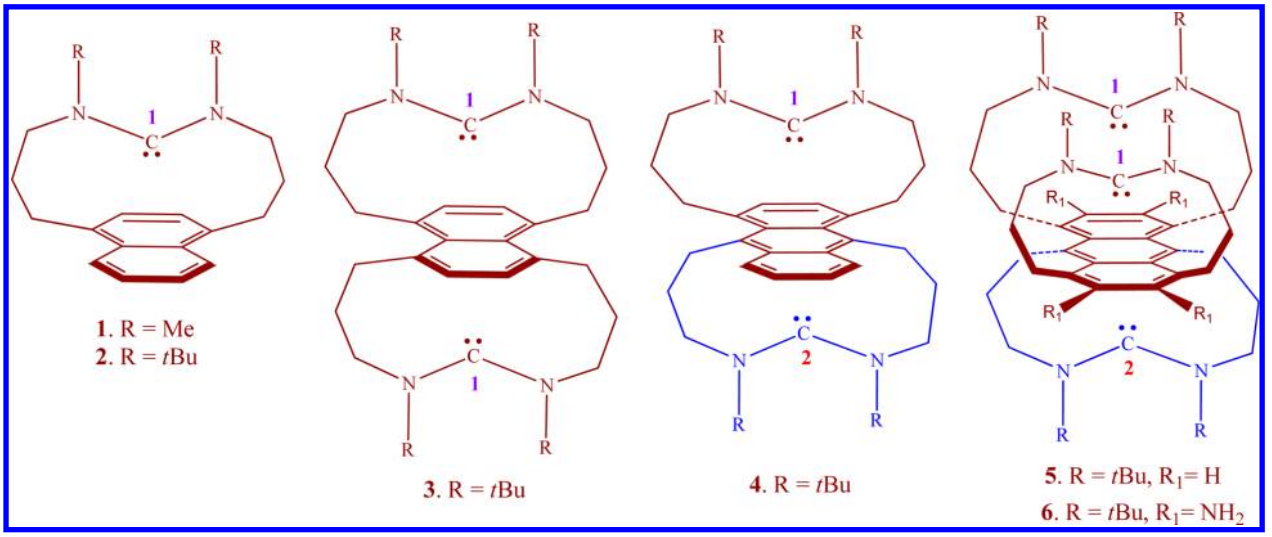

sible for the enhancement of the proton affinity for the systems by ∼30.0 kcal/mol.[40] We have utilized weak noncovalent interactions by using an acyclic carbene [:C(NR$_2$)$_2$] unit connects with the π-ring systems through propyl chains (Scheme 1). We have used napthalene and anthracene rings to design a new class of organic superbases through the C−H$^+$···π type interactions to achieve the hyperbasicity. This study will be helpful for achieving higher basicity by avoid of large functionalizations in the molecular scaffold of neutral organic superbases.[15,16,23−25,27]

These designed carbene superbases can be extended with independent bis- and tris-protonation sites in the same molecule (Scheme 1). There are a few reports available on the two independent protonation sites in a molecule.[8,17,19,21,33] The B3LYP/6-311+G**//B3LYP/6-31+G* calculated results suggest that third proton affinities for these carbene systems are greater than ∼300 kcal/mol in acetonitrile solvent medium. The higher level DFT calculated first proton affinity of the designed superbase is in the range of hyperbase (compounds that have a proton affinity >300 kcal mol^{-1}) in the gas phase.[16,17,27,41] Such neutral organic superbases can further be exploited as a molecular container for methane storage. Importantly, the synthesis of 1,4-bridged napthaleno- and anthracenophanes have been reported and their structure and reactivity has also been explored.[42−45] Such synthetic methods can be useful for experimentalists to prepare the designed organic superbases in the present study.

Natural gas (which mainly consists of methane) is considered as an alternative energy source due to the limitation of fossil fuels which maintain our daily life. The major problem in the field of methane storage is economic and consumes a considerable amount of energy while liquefying and compressing it.[46] A number of porous solids have been used in methane adsorption because of efficient gas−solid interaction and high methane storage capacities.[47−61] It has been reported that alkali-metal-containing zeolites and metal organic framework showed a high density of accessible strong adsorption toward methane.[51−57,59−64] The development of new material for methane storage has been considered an emergent interest in the field of materials chemistry.

We have shown that the multiple binding sites of a neutral organic superbase can be utilized for the storage of methane molecules. The carbene based scaffolds have the selective binding for small alkali metal cation, i.e., lithium ion and such molecular arrangements facilitate the spontaneous binding of methane with the electropositive lithium metal ions efficiently.

2. COMPUTATIONAL SECTION

The calculations were carried out for compounds **1**−**6** with the density functional theory using Becke's three-parameter hybrid functional with correlation formula of Lee, Yang, and Parr (B3LYP).[65,66] The carbenes were fully optimized with 6-31+G* basis set,[67] and harmonic vibrational frequency calculations were used to confirm the stationary points. The reliability of the B3LYP level for the calculations of the proton affinities for the divalent carbenes has been examined in the earlier report.[17] Single-point energies at the B3LYP/6-31+G* optimized geometries were calculated with B3LYP/6-311+G** level of theory. Further, we have employed M06-2X/6-311+G** level of theory to calculate the energies for these optimized carbene systems as M06-2X DFT functional considers the dispersion interactions more accurately for nonbonded interactions.[68]

Solvent effects were taken into account by means of the polarizable continuum model (PCM)[69−73] through single-point energy calculations at the B3LYP/6-311+G** level of theory (using the gas-phase optimized geometries). The pK_a value of the acid BH$^+$ was calculated using the following relation,

$$pK_a = \Delta G_{sol}/2.303RT$$

where

$$\Delta G_{sol} = \Delta G_{gas} + \Delta\Delta G_{solv} + \Delta G_{corr}$$

ΔG_{gas} is the Gibbs free energy change of the reaction in the gas phase and $\Delta\Delta G_{solv}$ is the difference in solvation free energies (ΔG_{solv}) between products and reactants. ΔG_{corr} is the correction associated to the change in standard state from gas phase (1 atm) to solution (1 mol/L), and its value at 298.15 K is 1.89 kcal/mol.[74]

Now ΔG_{sol} can be expressed as:

$$\Delta G_{sol} = G_{gas}(B) + \Delta G_{solv}(B) + G_{gas}(H^+) + \Delta G_{solv}(H^+) - G_{gas}(BH)^+ - \Delta G_{solv}(BH)^+ + 1.89$$

dx.doi.org/10.1021/jp5003319 | J. Phys. Chem. C 2014, 118, 6680−6689

Here, the value of Gibbs free energy of the proton in the gas phase was set to −6.28 kcal/mol using translational entropy calculated according to the well-known Sackur−Tetrode equation[75] and the value of Gibbs free energy of proton in acetonitrile solvent phase taken as −250.76 kcal/mol.[76]

The ΔG_{solv} values in B3LYP/6-31+G* optimized geometry with UAHF radii and 'scfvac' keyword used acetonitrile (ε = 36.64) as a solvent.[77,78] The reliability of this method for pK_a calculation has already been shown in earlier reports.[78] Both electrostatic and nonelectrostatic (i.e., cavitation, repulsion, and dispersion) terms were included in the calculation of ΔG_{solv} values.

The molecular electrostatic potential (MESP) was calculated using eq 1, where Z_A is the charge on nucleus A, situated at R_A, and $\rho(r')$ is the electron density.[79]

$$V(\mathbf{r}) = \sum_{A}^{N} \frac{Z_A}{|r - R_A|} - \int \frac{\rho(r')d^3r'}{|r - r'|} \quad (1)$$

In general, electron rich regions are shown by highly negative MESP, whereas electron deficient regions are characterized by positive MESP.[80−84] The most negative valued point (V_{min}) in electron rich regions can be determined from the MESP topography calculation.[85−87] Molecular electrostatic potential (MESP) calculations were performed at the M06-2X/6-311+G** level of theory.

The geometries are optimized at the M06-2X/6-31+G* level of theory for the lithium and sodium affinity calculations. We employed M06-2X/6-311+G** level of theory to calculate the energies for these optimized geometries. For the calculation of interaction energy per gas molecule (methane or H_2), the following expression was used,

interaction energy/gas molecule:

$$\Delta E = [E_{Complex} - (E_s + nE_{gas})]/n$$

desorption energy:

$$\Delta E_{DE} = E_{gas} + \left(\frac{1}{m}\right)[E_{S(gas)_{n-m}} - E_{S(gas)_n}]$$

where n, m = no. of gas molecules and S is the gas-trapped systems.

The absolute electronegativity (χ) and the absolute hardness (η) were calculated by the formula, χ = (IP + EA)/2 and η = (IP − EA), respectively.[21] The ionization potential (IP) was calculated as the energy difference between the nonoptimized cation-radical structure and the ground state structure, and the electron affinity (EA) was calculated as the energy difference between the anion-radical and ground state.

Electrophilicity (ω) is defined as

$$\omega = \frac{\chi^2}{2\eta}$$

Quantum chemical calculations were performed using the Gaussian 03, revision E.01 program,[88] while the calculations at M06-2X level were performed using the Gaussian 09 program.[89] The energy decomposition analysis was performed on these optimized geometries with the localized molecular orbital energy decomposition analysis (LMOEDA)[90] method as implemented in GAMESS.[91] M06-2X/6-31+G* level was used for LMOEDA calculations. In this energy decomposition analysis scheme, total interaction energy (ΔE_{int}) of the complex was decomposed into electrostatic (ΔE_{elec}), exchange (ΔE_{ex}), repulsion (ΔE_{rep}), polarization (ΔE_{pol}), and dispersion (ΔE_{disp}) components.[92,93]

$$\Delta E_{int} = \Delta E_{elec} + \Delta E_{ex} + \Delta E_{rep} + \Delta E_{pol} + \Delta E_{disp} \quad (2)$$

3. RESULTS AND DISCUSSION

The designed neutral organic superbases are illustrated in Scheme 1. We have calculated the proton affinities for these carbene systems with M06-2X/6-311+G** level of theory using the optimized geometries at the B3LYP/6-31+G* level of theory. M06-2X functional was considered as better model for the calculation of nonbonded interactions like C−H$^+$···π type as it considers the dispersion interactions more accurately. The calculated results suggest that the proton affinity values calculated at M06-2X level gives slightly lower value compared to the B3LYP level (Table 1). The calculated proton affinity of

Table 1. M06-2X/6-311+G//B3LYP/6-31+G* Calculated Proton Affinities (kcal/mol) for 1−6 in the Gas Phase at 298.15 K (B3LYP/6-311+G**//B3LYP/6-31+G* Calculated Proton Affinities Are Given in Parentheses)**

	proton affinity[a] (kcal/mol)		
compd	1st	2nd	3rd
1	277.2 [280.1]		
2	286.8 [288.3]		
3	291.3 [292.4]	243.6 [247.3]	
4	291.5 [292.4]	244.3 [247.9]	
5	295.6 [296.1]	250.7 [251.3]	197.0 [206.9]
6	301.9 [301.6]	255.6 [259.8]	202.0 [210.4]

[a]Zero-point energy corrected.

1 at M06-2X/6-311+G**//B3LYP/6-31+G* level of theory is 277.2 kcal/mol (Table 1). This calculated results suggest that carbene **1** possesses much higher proton affinity (PA) value than the proton affinity of a threshold organic superbase (compounds that have a PA > 1000 kJ mol^{-1} = 239 kcal mol^{-1}) and comparable with highly basic imines and phosphazene systems.[94,95] The role of arene ring systems to enhance the basicity in such carbene scaffolds is reflected from the calculated proton affinity values. The introduction of naphthalene ring connected with alkyl chains of simple :C(NMe$_2$)$_2$, enhances the proton affinity value by ∼8.6 kcal/mol compared to simple carbene :C(NMe$_2$)$_2$.[17] Similar proton stabilization occur in the protonated form of carbene systems containing a single phenyl ring which has been revealed from the calculated PA values.[17,21] The naphthalene moiety provides another protonation site in the system. The effect of substituents at the aminomethyl positions of carbene unit toward the enhancement of the proton affinity of **1** can be seen upon the introduction of *t*Bu groups at that positions (Scheme 1 and Table 1). The electron donating *t*Bu groups increases the electron density at the carbene carbon center through the inductive effect.[31] Molecular electrostatic potential (MESP) analysis supports this observation. The MESP analysis shows that *t*Bu groups increase the V_{min} value of the compound **2** (−91.0 kcal/mol) in the region between the carbene carbon and the phenyl ring compared to **1** (−87.1 kcal/mol) (Figure 1). The calculated PA value for **2** is 286.8 kcal/mol, which is 9.6 kcal/mol higher than that of **1** (Table 1).

We have introduced another carbene unit in **2** at the other naphthalene ring in the opposite direction to avoid steric

dx.doi.org/10.1021/jp5003319 | J. Phys. Chem. C 2014, 118, 6680−6689

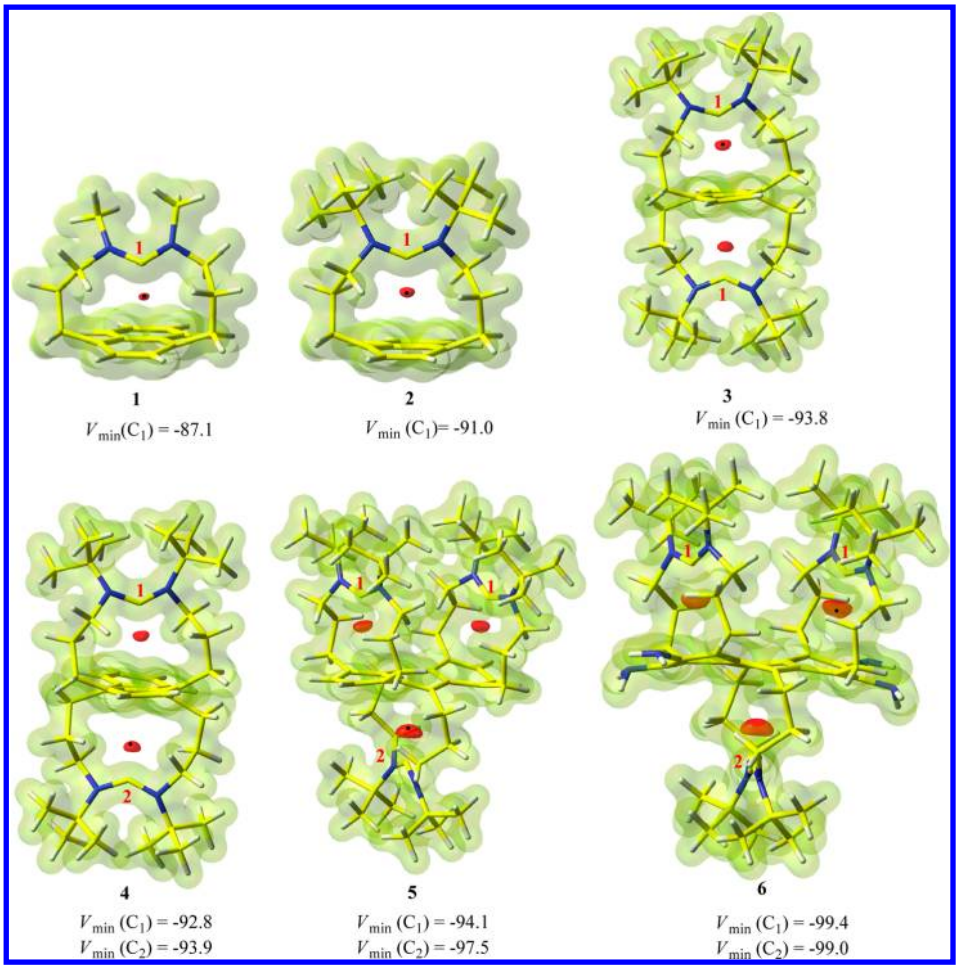

Figure 1. Representation of the MESP isosurface at −84.7 kcal/mol. The position of V_{min} is shown in black dots. All values are given in kcal/mol.

hindrance in the molecule (Scheme 1). This molecular scaffold enables for bis-protonation study. The other optimized geometry (**3′**) having two carbene units in the same side of the naphthalene ring is energetically 10.2 kcal/mol less stable than **3** at M06-2X/6-311+G**//B3LYP/6-31+G* level of theory. The instability caused in **3′** is due to severe steric strain in the system, which consequently deformed the naphthalene ring (Figure S1, Supporting Information). The two divalent carbon(II) units of **3** were protonated sequentially to obtain the first and second proton affinities. At first, we have calculated the proton affinity for one protonation site of **3** keeping the other protonation site in the deprotonated state. After that, the second protonation site is protonated with the first one in protonated state. By introducing the second carbene unit, the first proton affinity of the carbene **3** increases by 4.5 kcal/mol (Table 1). The MESP analysis shows that the V_{min} value is relatively higher in **3** (−93.8 kcal/mol) compared to **2** (−91.0 kcal/mol), which implies the existence of greater electron dense region over the carbene center in **3** (Figure 1). The second proton affinity value was found to be 243.6 kcal/mol (Table 1), which is higher than the proton affinity value of prototype DMAN molecule.[94]

We have extended our study with the anthracene ring in the place of the naphthalene ring (Scheme 1). As the two carbene units are in different environments, so we have performed MESP analysis to examine the existence of a greater electron dense region over the carbene center between these two carbene units (Figure 1). The calculated results show that the V_{min} value is relatively higher for the C2 carbene unit, which is connected with the middle ring of the anthracene molecule (Figure 1). We have optimized the geometry by protonating the C2 carbene unit to calculate the first proton affinity. The calculated first and second proton affinity values for **4** are similar to that of carbene **3** (Table 1). The third aromatic ring of the anthracene unit provides the tris-protonation site (Scheme 1). In carbene **5**, three carbene units are connected with each arene ring of anthracene molecule (Scheme 1). The optimized geometry of **5** shows that two carbene units are on the same side and other the carbene moiety is on the opposite side. The MESP analysis performed for **5** shows that the C2 carbene unit connecting with the middle ring has higher V_{min} value (−97.5 kcal/mol) than the other two carbene moieties (−94.1 kcal/mol) (Figure 1). We have first protonated the middle carbene unit followed by sequential protonation of other two carbene units. The calculated first proton affinity at M06-2X/6-311+G**//B3LYP/6-31+G* level of theory has been found to be 295.6 kcal/mol, which is ∼4.0 kcal/mol higher than the proton affinity value of carbene **3** and **4** (Table 1). The MESP analysis also shows that the V_{min} value (−97.5 kcal/mol) for **5** is much higher than the carbenes **3** (−93.8 kcal/mol) or **4** (−93.9 kcal/mol) (Figure 1). Furthermore, there is a significant increase in the second proton affinity value for carbene **5**. The second proton affinity value increases by ∼6.0 kcal/mol compared to **3** and **4** (Table 1). The calculated third proton affinity has been found to be 197.0 kcal/mol, which is comparable to normal base.

dx.doi.org/10.1021/jp5003319 | J. Phys. Chem. C 2014, 118, 6680−6689

We have examined the role of suitable electron donating substituents on the phenyl rings of anthracene molecule to enhance the basicity of the systems. We have substituted four $-NH_2$ groups in the anthracene molecule as electron donating substituents (Scheme 1). The presence of such electron releasing groups can triggered the basicity of the system by considerable stabilization of the cationic form. The combined effect of induction and π-electron conjugation of the amine group influences increase of the electron density over the π cloud of the anthracene ring.[96] The MESP analysis also shows that there is an increase of electron rich region over the C1 carbene units than the middle C2 carbene unit (Figure 1). One of the side carbene moieties is protonated first, followed by sequential protonation of other two carbene units. The role of electron donating $-NH_2$ groups in the anthracene ring is reflected on the calculated proton affinity values for **6** at M06-2X/6-311+G**//B3LYP/6-31+G* level of theory. The first PA value for **6** has been found to be higher compared to **5** by 6.0 kcal/mol (Table 1). Carbene **6** showed the PA value of 301.9 kcal/mol, which is the range of hyperbase (compounds that have a proton affinity >300 kcal mol^{-1})[16,17,27,41] (Table 1). The calculated second and third proton affinity values of **6** are 255.6 and 202.0 kcal/mol, respectively. The second proton affinity value is found to be similar compared to the reported PAs of NHCs.[97]

The MESP results show that the electron rich region increases on going from **1** to **6** (Figure 1). The PA values for these compounds correlate well with the V_{min} values (Figure S2, Supporting Information).

We have calculated the pK_a and proton affinity values of the designed superbases (**1**−**6**) using the polarized continuum model (PCM) in MeCN. The calculated proton affinities are much higher in (MeCN) than in the gas phase.[98] The greater stability of the conjugate acid in a polar solvent medium than the initial base is responsible for such higher basicity. That all the proton affinities are greater than 300.0 kcal/mol indicates their strong basicity in acetonitrile medium (Table 2). The greater stabilization of the bis- and tris-cationic forms of carbenes in the solvent medium compared to the corresponding neutral and monocationic forms contributes more to enhance the second and third proton affinity values of such systems.[21,99] The third proton affinity value for **6** is 312.1 kcal/mol, which is much higher than the PA(MeCN) values of normal bases like NH_3 (275.0 kcal/mol), $N(Me)_3$ (277.6 kcal/mol), and $N(Et)_3$ (278.6 kcal/mol).[98] We have further determined the pK_a values for such carbene superbases (**1**−**6**) (Table 2). The reliability of the method for the pK_a of carbene superbases has been examined against the available experimental data.[17] The calculated pK_a value of **1** is 42.7, which is much higher than the experimental pK_a value of DMAN (18.5).[100] The calculated results show that the highly basic carbene **6** exhibits a pK_a of 52.0, which is 33 orders of magnitude stronger than DMAN (Table 2).[100] The second pK_a value is reported for the designed superbases up to 48.4, whereas the third pK_a value is 43.3. Such higher pK_a value for the third protonation is much higher than the experimental pK_a values of normal bases such as NH_3 (16.46) and $N(Me)_3$ (17.6).[98] A good correlation between calculated PA (MeCN) and pK_a values was observed with high correlation coefficient value of 0.98 (Figure S3, Supporting Information). It has to be mentioned that some variations might occur in the calculated and experimentally determined pK_a values as the solvation appears to affect the $C-H^+\cdots\pi$ interactions.[101]

We have calculated the singlet and triplet energy gap ($E_{S\text{-}T}$) at M06-2X/6-311+G**//B3LYP/6-31+G* level of theory of the carbene systems in the gas phase. The energy gap signifies the nature and strength of the carbene systems. The calculated singlet and triplet energy gap (E_{S-T}) for **1** is found to be 60.4 kcal/mol, which signifies the greater stability of singlet state over triplet state (Table S1, Supporting Information). Furthermore, we have computed the singlet and triplet states energy difference for **2**, **3**, and **5**. The greater preference of singlet state over triplet state is observed for these designed carbene superbases also (Table S1, Supporting Information).[102]

The energies of the HOMO and LUMO levels in the carbenes also suggest the reactivity and stability of these systems. The orbital pictures show that the lone pair is localized on the central carbon atom of the carbene units in the highest occupied molecular orbital (HOMO) (Figure S4, Supporting Information). Compound **6** shows the highest HOMO energy (−5.12 eV) in the series, which predicts its higher reactivity than the other studied carbene scaffolds (Table S2, Supporting Information). The highest proton affinity value for **6** in this series also supports this observation (Table 1). A good correlation between calculated PA and E_{HOMO} was observed with high correlation coefficient value of 0.95 (Figure 2).

Table 2. B3LYP/6-311+G//B3LYP/6-31+G* Calculated Proton Affinities (kcal/mol) and pK_a (MeCN) for 1−6 in the Acetonitrile Medium at 298.15 K**

	proton affinity[a] (kcal/mol)			pKa
compd	1st	2nd	3rd	
1	314.0			42.7
2	318.9			46.5
3	320.2	316.5		47.9, 45.3
4	319.1	315.8		47.1, 44.5
5	320.6	315.9	309.0	47.8, 44.3, 41.4
6	325.8	321.3	312.1	52.0, 48.4, 43.3

[a]Zero-point energy corrected.

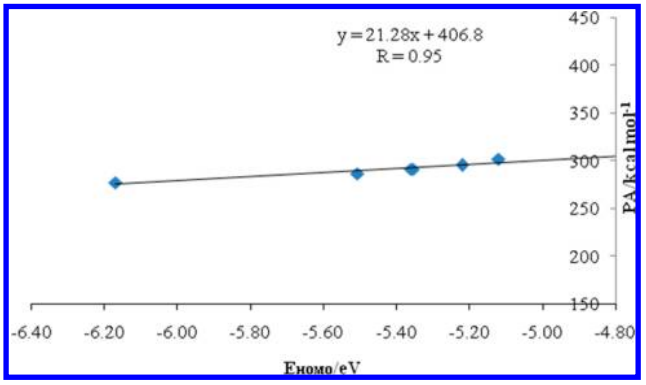

Figure 2. Correlation between calculated PA in gas phase and E_{HOMO} of carbene bases.

The M06-2X/6-311+G**//B3LYP/6-31+G* calculated results indicate that the designed carbene systems possess very higher basicity and can be used as efficient reagents in organic synthesis, green chemistry, etc.[1−3] We have explored the possibility of these carbene superbases as an effective storage materials for hydrogen which is implemented in earlier study.[21] We have shown the utilization of such carbene superbases for

dx.doi.org/10.1021/jp5003319 | J. Phys. Chem. C 2014, 118, 6680−6689

selective binding of lithium ions over sodium ions and the use of such lithiated superbase for effective storage materials for hydrogen. The designed carbenes have multiple binding sites and can accommodate a number of hydrogen molecules. We have performed the geometrical analysis for these carbenes, and the geometrical parameters show that the distance between the carbene carbon and the center of the phenyl ring is in the range of 3.200−3.900 Å. This space is suitable for the accommodation of the smallest alkali metal ion, i.e., Li^+ (ionic radius 0.76 Å), and can have efficient cation−π interaction with the phenyl ring. The calculated binding energies at M06-2X/6-311+G**//M06-2X/6-31+G* level of theory suggest that these carbene scaffolds have strong affinity to bind with lithium ion (Table 3).

Table 3. Complexation Energies of Different Carbenes at M06-2X/6-311+G//M06-2X/6-31+G* Level of Theory (Energies in kcal/mol)**

carbenes	BE (Li^+)	BE (Na^+)	ΔE (Li^+/Na^+)
1	−78.8	−54.0	24.8
2	−84.2	−62.1	22.1
3	−93.2	−80.3	12.9
3 (Bis)	−24.1	−1.3	22.8
4	−93.4	−86.4	7.0
4 (Bis)	−26.9	−6.1	20.8

The importance of phenyl ring in stabilizing the lithium ion binding energy calculated for **1** is revealed through the calculation of simple carbene $:C(NMe_2)_2$ with Li^+ ion. The calculated results suggest that the phenyl ring gives additional stability of Li^+ binding with **1** by 19 kcal/mol. The NBO charge analysis also shows the higher positive charge on lithium center compared to carbon atom, which results C−Li bond polar in nature (Table S3, Supporting Information). We have also computed the binding affinity of sodium cation (ionic radius 1.02 Å), and the calculated results showed much lower binding energies than the lithium ion with these carbene systems (Table 3). The higher preference of Li^+ ion with these carbene scaffolds encouraged us to examine the adsorption of hydrogen molecules with these lithiated organic superbases.

We have examined the interactions of hydrogen molecules with the lithiated carbene compounds (**1**−**3**). The optimized geometries are given in Figure 3. The M06-2X/6-311+G**//M06-2X/6-31+G* calculated results show that the lithiated carbene **1** interacted with hydrogen molecule with an interaction energy of −3.7 kcal/mol per H_2 molecule (Table 4). The geometrical parameters show that the hydrogen molecule lies at a distance of 2.11 Å from the Li^+ ion in the lithiated carbene **1** (Figure 3a and Table S4, Supporting Information). In carbene **3**, we have examined the possibility of hydrogen adsorption with two molecular hydrogens (Figure 3b).

The presence of a high positive charge on the Li ion favors the trapping of hydrogen molecule in these cases through ion-quadrupole and ion-induced dipole interactions.[103−105] Herein, we have adopted a new strategy for exploiting these lithiated carbene derivatives as materials for methane storage. The lithiated carbenes **1**−**3** have been examined for methane storage materials. The optimized methane trapped lithiated carbenes (**1**) are given in Figure 4. The calculated results show that the lithiated carbene **1** interacted with molecular methane with a binding energy of −6.7 kcal/mol per methane molecule, which is relatively higher than the binding energy of H_2

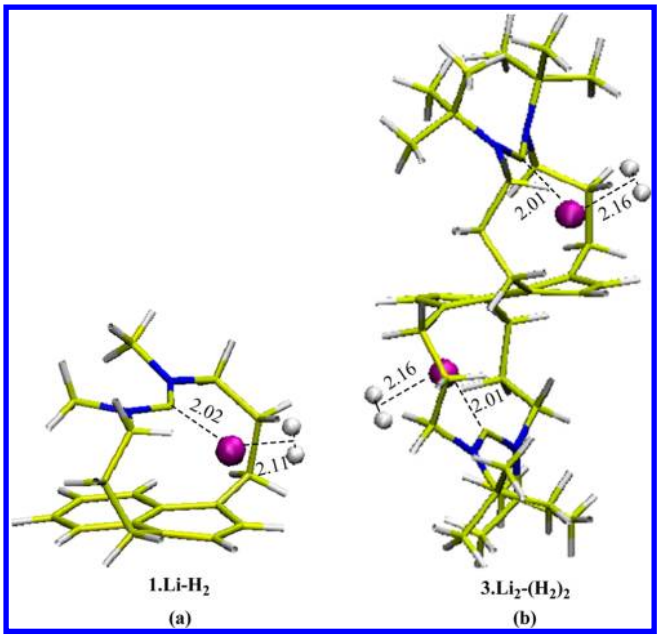

Figure 3. Geometries of hydrogen trapped lithiated carbene at M06-2X/6-31+G* level of theory. Distances are in Å (yellow = carbon, blue = nitrogen, pink = lithium, and white = hydrogen).

Table 4. Interaction Energy (ΔE) and Desorption Energy (ΔE_{DE}) per Hydrogen Molecule for Hydrogen Trapped Lithiated Carbenes at M06-2X/6-311+G//M06-2X/6-31+G* Level of Theory[a]**

	ΔE	ΔE_{DE}
1·Li + H_2 = **1**·Li−H_2	−3.7 (−2.98)	3.7
2·Li + H_2 = **2**·Li−H_2	−1.8 (−1.60)	1.8
3·Li_2 + 2H_2 =**3**·Li_2-$(H_2)_2$	−2.9 (−3.45)	2.9

[a]Energies are in kcal/mol. BSSE corrected interaction energies at M06-2X/6-31+G* level of theory are given in parentheses.

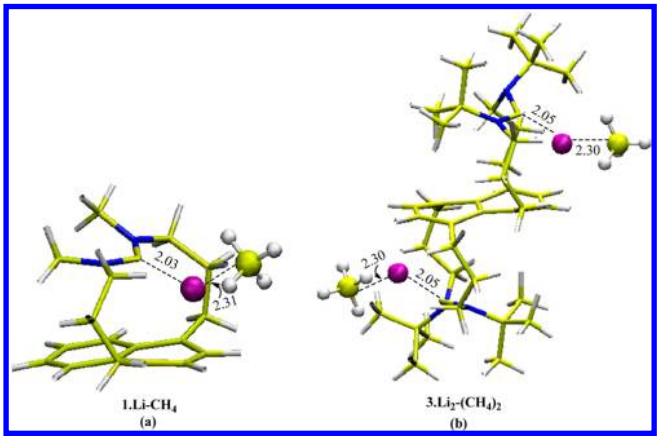

Figure 4. Geometries of methane trapped lithiated carbenes at M06-2X/6-31+G* level of theory. Distances are in Å (yellow = carbon, blue = nitrogen, pink = lithium, and white = hydrogen).

molecule (Table 5). The presence of a higher positive charge on Li ion helps to trap the methane molecule favorably (Table S3, Supporting Information).[106] The optimized geometry shows that the methane molecule positioned at a distance of 2.31 Å from the Li^+ ion (Figure 4a and Table S5, Supporting Information). In the lithiated carbene **3**, we have explored the possibility of methane adsorption with two molecular methane

dx.doi.org/10.1021/jp5003319 | J. Phys. Chem. C 2014, 118, 6680−6689

Table 5. Interaction Energy (ΔE) and Desorption Energy (ΔE_{DE}) per methane Molecule for Methane Trapped Lithiated Carbenes at M06-2X/6-311+G//M06-2X/6-31+G* Level of Theory[a]**

	ΔE	ΔE_{DE}
1·Li + CH_4 = **1**·Li-CH_4	−6.7 (−6.92)	6.7
2·Li + CH_4 = **2**·Li-CH_4	−7.2 (−7.09)	7.2
3·Li_2 + 2CH_4 =**3**·Li_2-$(CH_4)_2$	−8.8 (−8.27)	8.8

[a]Energies are in kcal/mol. BSSE corrected interaction energies at M06-2X/6-31+G* level of theory are given in parentheses.

(Figure 4b). The calculated interaction energy is much higher for lithiated carbene **3** compared to **1** and **2** (Table 5). NBO charge analysis also showed that the positive charge on lithium ion is reduced in the methane trapped molecules (Table S6, Supporting Information). This study was extended with the single lithium ion to gauge the interaction of gases with lithiated carbene systems. The calculated results show that the interaction energy of single lithium ion adsorbed methane molecule is −11.9 kcal/mol at M06-2X/6-31+G* level of theory, which is nearly comparable to the lithiated carbene **3** (Table 5 and Figure S5, Supporting Information). The recyclable property of gas storage materials also depends on the desorption energy (ΔE_{DE}). The lower desorption energy (ΔE_{DE}) calculated for lithiated carbenes indicates that these systems can be used as a good recyclable gas storage materials (Table 5 and Figure S5, Supporting Information).[103]

We have performed the global reactivity descriptors calculation to analyze the stability of methane trapped molecules according to both the maximum hardness principle and the minimum electrophilicity principle.[107,108] We have calculated the hardness (η) and electrophilicity (ω) values for lithiated carbene systems before and after methane trapping process. After methane binding, there is an increase of hardness (η) value for the lithiated carbene **1** and electrophilicity (ω) value is decreased, which facilitates the methane trapping process (Table S7, Supporting Information).

We have performed the energy decomposition analysis (EDA) scheme to investigate the physical origins of such interactions. The localized molecular orbital energy decomposition analysis method (LMO-EDA) as implemented in the quantum chemistry software GAMESS is carried out to examine the factors contributing to such interaction energies.[90,91] The total interaction energy is decomposed into electrostatic, exchange, repulsion, polarization, and dispersion components. The energy decomposition is analyzed at the M06-2X level in conjugation with 6-31+G* level of theory (Table 6). The calculated results of methane trapped carbene **1** showed that the total interaction energy (ΔE_{int}) is −6.91 kcal/mol, which is similar to the BSSE corrected interaction energy

Table 6. LMOEDA Decomposed Energy Terms in kcal/mol at M06-2X/6-31+G* Level of Theory

	1·Li-CH_4	**1**·Li−H_2
electrostatic	−4.24	−1.67
exchange	−3.40	−1.16
repulsion	14.29	5.81
polarization	−4.33	−1.99
dispersion	−9.23	−3.97
total	**−6.91**	**−2.98**

calculated with Gaussian 09 program (Table 5 and 6). In methane complexed carbene **1**, the attractive interactions are electrostatic (−4.24 kcal/mol), exchange (−3.40 kcal/mol), polarization (−4.33 kcal/mol), and dispersion interaction (−9.23 kcal/mol). The destabilization due to the repulsion is much larger (14.29 kcal/mol) than the exchange stabilization (−3.40 kcal/mol). The closed shell interactions from dispersion, exchange, and repulsion terms contributed of 1.66 kcal/mol to the total interaction energy (Table 6). The ΔE_{int} is therefore approximately equal to electrostatic (−4.24 kcal/mol) and polarization (−4.33 kcal/mol). Therefore, the electrostatic and polarization interactions make significant contributions (−8.57 kcal/mol). These calculated results suggest that the interaction is mainly due to a cation-induced dipole electrostatic interaction.[106] Further, it is supported from the SCF deformation density isosurface generated for methane trapped lithiated carbene **1** (Figure 5). This density deformation density

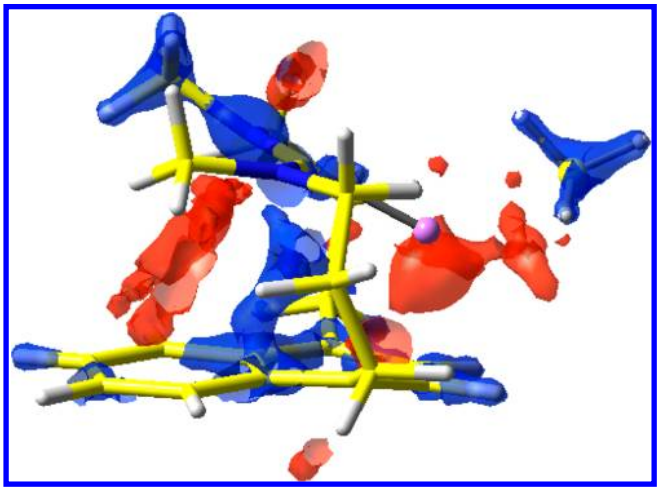

Figure 5. SCF deformation density isosurfaces (set to 0.22) from fragment analysis of methane trapped lithiated carbene **1**.

also diminishes the probability of σ-donation from methane C−H bonds to lithium ion.[106] Further, we have extended the study with performing the energy decomposition analysis for hydrogen trapped carbene **1** at M06-2X/6-31+G* level of theory (Table 6). The calculated results suggest that the electrostatic and polarization interactions make largest contributions (−3.66 kcal/mol) to the total interaction energy similar to the interaction of methane molecule with such lithiated carbenes (Table 6).

4. CONCLUSIONS

In this work, we report the multiprotonation sites exploiting noncovalent interactions to achieve hyperbasicity of a neutral organic base. A new class of carbene based organic superbase has been designed to attain the proton affinity (PA) value of 301.9 kcal/mol at the M06-2X/6-311+G**//B3LYP/6-31+G* level of theory. These designed scaffold molecules possess three independent protonation sites, which is not available in the literature to date. The stabilization of the protonated forms of the superbases by noncovalent interactions such as C−H^+···π interaction is responsible for augmenting the basicity of such carbene systems. The DFT calculated results show that such carbene systems can be suitable candidates for tris-protonation, with a pK_a(MeCN) value of 43.3 and proton affinity value (MeCN) of 312.1 kcal/mol. Molecular electrostatic potential

dx.doi.org/10.1021/jp5003319 | J. Phys. Chem. C 2014, 118, 6680−6689

(MESP) analysis shows the existence of electron density at the reactive sites and the role of substituents to enhance the electron density in such designed systems. The absolute minima of the MESP (V_{min}) located for such carbene systems correlated well with their calculated proton affinity values. The frontier molecular orbital energy of such carbenes also shows a good relationship with their proton affinity results. This is an example where we have shown that these superbases can be exploited as molecular containers for the storage of multiple methane molecules. The global reactivity descriptors show the stability of these methane trapped molecules. The localized molecular orbital energy decomposition reveals the role of the factors contributing to the interaction energy. We hope that this information will stimulate chemists to exploit the use of organic superbases for natural gas like methane storage materials besides their many other applications.

■ ASSOCIATED CONTENT

Supporting Information

Cartesian coordinates of all the geometries, including electronic energies. This material is available free of charge via the Internet at http://pubs.acs.org.

■ AUTHOR INFORMATION

Corresponding Author

*Phone: +91-278-2567760 ext 6770. Fax: (+91)-278-2567562. E-mail: ganguly@csmcri.org.

Notes

The authors declare no competing financial interest.

■ ACKNOWLEDGMENTS

R.L. is thankful to UGC, New Delhi, India, for awarding senior research fellowship. B.G. thanks MSM, SIP, CSIR, New Delhi, and DST, New Delhi, for financial support. We are also thankful to the reviewers for their suggestions and comments that have helped us to improve the paper.

■ REFERENCES

(1) *Superbases for Organic Synthesis*; Ishikawa, T., Ed.; Wiley: Chichester, West Sussex, 2009.

(2) Hirono, Y.; Kobayashi, K.; Yonemoto, M.; Kondo, Y. Metal-free Deprotonative Functionalization of Heteroaromatics using Organic Superbase Catalyst. *Chem. Commun.* **2010**, *46*, 7623−7624 and references therein..

(3) Vazdar, K.; Kunetskiy, R.; Saame, J.; Kaupmees, K.; Leito, I.; Jahn, U. Very Strong Organosuperbases Formed by Combining Imidazole and Guanidine Bases: Synthesis, Structure, and Basicity. *Angew. Chem., Int. Ed.* **2014**, *53*, 1435−1438.

(4) Oediger, H.; Mőller, F.; Eiter, K. Bicyclic Amidines as Reagents in Organic Syntheses. *Synthesis* **1972**, 591−598.

(5) Tang, J.; Dopke, J.; Verkade, J. G. Synthesis of New Exceedingly Strong Non-ionic Bases: RN:P(MeNCH$_2$CH$_2$)$_3$N. *J. Am. Chem. Soc.* **1993**, *115*, 5015−5020 and references therein..

(6) Ishikawa, T.; Isobe, T. Modified Guanidines as Chiral Auxiliaries. *Chem.—Eur. J.* **2002**, *8*, 552−557.

(7) Bachrach, S. M.; Wilbanks, C. C. Using the Pyridine and Quinuclidine Scaffolds for Superbases: A DFT Study. *J. Org. Chem.* **2010**, *75*, 2651−2660.

(8) Estrada, E.; Simón-Manso, Y. Rational Design and First Principles Studies Toward the Discovery of a Small and Versatile Proton Sponge. *Angew. Chem., Int. Ed.* **2006**, *45*, 1719−1721.

(9) Maksić, Z. B.; Kovačević, B.; Vianello, R. Advances in Determining the Absolute Proton Affinities of Neutral Organic Molecules in the Gas Phase and Their Interpretation: A Theoretical Account. *Chem. Rev.* **2012**, *112*, 5240−5270.

(10) Singh, A.; Ganguly, B. DFT Studies toward the Design and Discovery of a Versatile Cage-Functionalized Proton Sponge. *Eur. J. Org. Chem.* **2007**, 420−422.

(11) Singh, A.; Ganguly, B. Strategic Design of Small and Versatile Bicyclic Organic Superbases: A Density Functional Study. *New J. Chem.* **2008**, *32*, 210−213.

(12) Singh, A.; Ganguly, B. Rational Design and First-Principles Studies toward the Remote Substituent Effects on a Novel Tetracyclic Proton Sponge. *J. Phys. Chem. A.* **2007**, *111*, 6468−6471.

(13) Maksić, Z. B.; Kovačević, B. Absolute proton affinity of some polyguanides. *J. Org. Chem.* **2000**, *65*, 3303−3309.

(14) Vianello, R.; Kovačević, B.; Maksić, Z. B. In Search of Neutral Organic Superbases—Iminopolyenes and their Amino Derivatives. *New J. Chem.* **2002**, *26*, 1324−1328.

(15) Margetić, D.; Ishikawa, T.; Kumamoto, T. Exceptional Superbasicity of Bis(guanidine) Proton Sponges Imposed by the Bis(secododecahedrane) Molecular Scaffold: A Computational Study. *Eur. J. Org. Chem.* **2010**, 6563−6572 and references therein..

(16) Peran, N.; Maksić, Z. B. Polycyclic Croissant-like Organic Compounds are Powerful Superbases in the Gas phase and Acetonitrile—A DFT Study. *Chem. Commun.* **2011**, *47*, 1327−1329.

(17) Lo, R.; Ganguly, B. First Principle Studies toward the Design of a New Class of Carbene Superbases Involving Intramolecular H$\cdots\pi$ Interactions. *Chem. Commun.* **2011**, *47*, 7395−7397.

(18) Lo, R.; Ganguly, B. Exploiting Propane-1,3-diimines as Building Blocks for Superbases: A DFT study. *New J. Chem.* **2011**, *35*, 2544−2550.

(19) Lo, R.; Singh, A.; Kesharwani, M. K.; Ganguly, B. Rational Design of A New Class of Polycyclic Organic Bases Bearing Two Superbasic Sites and Their Applications in the CO_2 Capture and Activation Process. *Chem. Commun.* **2012**, *48*, 5865−5867.

(20) Biswas, A. K.; Lo, R.; Ganguly, B. First Principles Studies toward the Design of Silylene Superbases: A Density Functional Theory Study. *J. Phys. Chem. A* **2013**, *117*, 3109−3117.

(21) Lo, R.; Ganguly, B. Is Noncovalent Interactions sufficient for Paracyclophane Based Carbenes to Achieve the Dual Properties: Hyperbasicity and Multiple Dihydrogen Storage Materials? A First Principles Study. *J. Phys. Chem C* **2013**, *117*, 19325−19333.

(22) Biswas, A. K.; Lo, R.; Ganguly, B. Is the Isodesmic Reaction Approach a Better Model for Accurate Calculation of pK_a of Organic Superbases? A Computational Study. *Synlett* **2013**, *24*, 2519−2524.

(23) Kovačević, B.; Barić, D.; Maksić, Z. B. Basicity of Exceedingly Strong Non-ionic Organic Bases in Acetonitrile—Verkade's Superbase and Some related Phosphazenes. *New J. Chem.* **2004**, *28*, 284−288.

(24) Kovačević, B.; Maksić, Z. B. High Basicity of Tris-(tetramethylguanidinyl)-phosphine Imide in the Gas Phase and Acetonitrile—A DFT Study. *Tetrahedron Lett.* **2006**, *47*, 2553−2555.

(25) Kovačević, B.; Maksić, Z. B. High Basicity of Phosphorus−Proton Affinity of Tris-(tetramethylguanidinyl)phosphine and Tris-(hexamethyltriaminophosphazenyl)phosphine by DFT Calculations. *Chem. Commun.* **2006**, 1524−1526.

(26) Schwesinger, R.; Hasenfratz, C.; Schlemper, H.; Walz, L.; Peters, E.-M.; Peters, K.; von Schnering, H. G. How Strong and How Hindered Can Uncharged Phosphazene Bases Be? *Angew. Chem., Int. Ed.* **1993**, *32*, 1361−1363.

(27) Despotović, I.; Kovačević, B.; Maksić, Z. B. Hyperstrong Neutral Organic Bases: Phosphazeno Azacalix[3](2,6)pyridines. *Org. Lett.* **2007**, *9*, 4709−4712.

(28) Despotović, I.; Maksić, Z. B.; Vianello, R. Design of Brønsted Neutral Organic Bases and Superbases by Computational DFT Methods: Cyclic and Polycyclic Quinones and [3]Carbonylradialenes. *Eur. J. Org. Chem.* **2007**, 3402−3413 and references therein..

(29) Kovačević, B.; Despotović, I.; Maksić, Z. B. In Quest Of Strong Neutral Organic Bases And Superbases—Supramolecular Systems Containing Four Pyridine Subunits. *Tetrahedron Lett.* **2007**, *48*, 261−264.

(30) Bucher, G. DFT Calculations on a New Class of C_3-Symmetric Organic Bases: Highly Basic Proton Sponges and Ligands for Very Small Metal Cations. *Angew. Chem., Int. Ed.* **2003**, *42*, 4039−4042.

(31) Maksić, Z. B.; Glasovac, Z.; Despotović, I. Predicted High Proton Affinity Of Poly-2,5-Dihydropyrrolimines—The Aromatic Domino Effect. *J. Phys. Org. Chem.* **2002**, *15*, 499−508.
(32) Alder, R. W. Design Of C_2-Chiral Diamines That Are Computationally Predicted To Be A Million-Fold More Basic Than The Original Proton Sponges. *J. Am. Chem. Soc.* **2005**, *127*, 7924−7931.
(33) Coles, M. P.; Aragón-Sáez, P. J.; Oakley, S. H.; Hitchcock, P. B.; Davidson, M. G.; Maksić, Z. B.; Vianello, R.; Leito, I.; Kaljurand, I.; Apperley, D. C. Superbasicity of a Bis-guanidino Compound with a Flexible Linker: A Theoretical and Experimental Study. *J. Am. Chem. Soc.* **2009**, *131*, 16858−16868.
(34) Jessop, P. G.; Heldebrant, D. J.; Li, X. W.; Eckert, C. A.; Liotta, C. L. Reversible Nonpolar-To-Polar Solvent. *Nature* **2005**, *436*, 1102−1102.
(35) Heldebrant, D. J.; Koech, P. K.; Rainbolt, J. E.; Zheng, F.; Smurthwaite, T.; Freeman, C. J.; Oss, I. Leito, Performance Of Single-Component CO_2-Binding Organic Liquids (CO_2BOLs) For Post Combustion CO_2 Capture. *Chem. Eng. J.* **2011**, *171*, 794−800.
(36) D. J. Heldebrant, M.; Yonker, C. R.; Jessop, P. G.; Phan, L. Organic Liquid CO_2 Capture Agents With High Gravimetric CO_2 Capacity. *Energy Environ. Sci.* **2008**, *1*, 487−493.
(37) Yang, Z.; He, L.; Zhao, Y.; Li, B.; Yu, B. CO_2 Capture And Activation By Superbase/Polyethylene Glycol And Its Subsequent Conversion. *Energy Environ. Sci.* **2011**, *4*, 3971−3975.
(38) Lo, R.; Ganguly, B. Efficacy Of Carbenes For CO_2 Chemical Fixation And Activation By Their Superbasicity/Alcohol: A DFT Study. *New J. Chem.* **2012**, *36*, 2549−2554.
(39) Wang, C.; Luo, X.; Luo, H.; Jiang, D.; Li, H.; Dai, S. Tuning the Basicity of Ionic Liquids for Equimolar CO_2 Capture. *Angew. Chem., Int. Ed.* **2011**, *50*, 4918−4922 and references therein..
(40) Zheng, F.; Sa, R.; Cheng, J.; Jiang, H.; Shen, J. Carbocation−π Interaction With Car−Parrinello Molecular Dynamics: Ab Initio Molecular Dynamics Investigation Of Complex Of Methyl Cation With Benzene. *Chem. Phys. Lett.* **2007**, *435*, 24−28.
(41) Vianello, R.; Maksić, Z. B. Rees Polycyanated Hydrocarbons and Related Compounds Are Extremely Powerful Brønsted Superacids in the Gas-Phase And DMSO—A Density Functional B3LYP Study. *New J. Chem.* **2008**, *32*, 413−427.
(42) Tobe, Y.; Saiki, S.; Naemura, K. A New Entry To [6](1,4)Napthalenophane and [6](1,4)Anthracenophane: Synthesis Of Peri-Substituted Derivatives. *Tetrahedron Lett.* **1995**, *35*, 939−942.
(43) Tobe, Y.; Saiki, S.; Minami, H.; Naemura, K. Synthesis and Structure of [6](1,4)Napthalenophane and [6](I,4)Anthracenophane and Their Peri-Substituted Derivatives. *Bull. Chem. Soc. Jpn.* **1997**, *70*, 1935−1942.
(44) Tobe, Y.; Saiki, S.; Utsumi, N.; Kusumoto, T.; Ishii, H.; Kakiuchi, K.; Kobiro, K.; Naemura, K. Synthesis, Characterization, and Molecular Structure of [6](9,10)Anthracenophane and Its Peri-Substituted Derivatives: The Smallest 9,10-Bridged Anthracenes. *J. Am. Chem. Soc.* **1996**, *118*, 9488−9497.
(45) Tobe, Y.; Takemura, A.; Jimbo, M.; Takahashi, T.; Kobiro, K.; Kakiuchi, K. Unusual Reactivity of Bent Acenes: Reactions of [6](1,4)Naphthalenophane and [6](1,4)Anthracenophane with Electrophiles. *J. Am. Chem. Soc.* **1992**, *114*, 3479−3491.
(46) Sillar, K.; Sauer, J. Ab Initio Prediction of Adsorption Isotherms for Small Molecules in Metal−Organic Frameworks: The Effect of Lateral Interactions for Methane/CPO-27-Mg. *J. Am. Chem. Soc.* **2012**, *134*, 18354−18365.
(47) Chae, H. K.; Siberio-Perez, D. Y.; Kim, J.; Go, Y.; Eddaoudi, M.; Matzger, A. J.; O'Keeffe, M.; Yaghi, O. M. A Route to High Surface Area, Porosity and Inclusion of Large Molecules In Crystals. *Nature* **2004**, *427*, 523−527.
(48) Ferey, G.; Mellot-Draznieks, C.; Serre, C.; Millange, F.; Dutour, J.; Surble, S.; Margiolaki, I. A Chromium Terephthalate-Based Solid with Unusually Large Pore Volumes and Surface Area. *Science* **2005**, *309*, 2040−2042.
(49) Farha, O. K.; Yazaydın, A. Ö.; Eryazici, I.; Malliakas, C. D.; Hauser, B. G.; Kanatzidis, M. G.; Nguyen, S. T.; Snurr, R. Q.; Hupp, J. T. De Novo Synthesis Of A Metal−Organic Framework Material Featuring Ultrahigh Surface Area and Gas Storage Capacities. *Nature Chem.* **2010**, *2*, 944−948.
(50) Furukawa, H.; Ko, N.; Go, Y. B.; Aratani, N.; Choi, S. B.; Choi, E.; Yazaydin, A. Ö.; Snurr, R. Q.; O'Keeffe, M.; Kim, J.; Yaghi, O. M. Ultrahigh Porosity in Metal−Organic Frameworks. *Science* **2010**, *329*, 424−428.
(51) Eddaoudi, M.; Kim, J.; Rosi, N.; Vodak, D.; Wachter, J.; O'Keeffe, M.; Yaghi, O. M. Systematic Design of Pore Size and Functionality in Isoreticular MOFs and Their Application in Methane Storage. *Science* **2002**, *295*, 469−472.
(52) Bourrelly, S.; Llewellyn, P. L.; Serre, C.; Millange, F.; Loiseau, T.; Ferey, G. Different Adsorption Behaviors of Methane and Carbon Dioxide in the Isotypic Nanoporous Metal Terephthalates MIL-53 and MIL-47. *J. Am. Chem. Soc.* **2005**, *127*, 13519−13521.
(53) Ma, S.; Sun, D.; Simmons, J. M.; Collier, C. D.; Yuan, D.; Zhou, H.-C. Metal−Organic Framework from an Anthracene Derivative Containing Nanoscopic Cages Exhibiting High Methane Uptake. *J. Am. Chem. Soc.* **2008**, *130*, 1012−1016.
(54) Wu, H.; Zhou, W.; Yildirim, T. High-Capacity Methane Storage in Metal−Organic Frameworks M2(dhtp): The Important Role of Open Metal Sites. *J. Am. Chem. Soc.* **2009**, *131*, 4995−5000.
(55) Dietzel, P. D. C.; Besikiotis, V.; Blom, R. Application of Metal−Organic Frameworks with Coordinatively Unsaturated Metal Sites in Storage and Separation of Methane and Carbon Dioxide. *J. Mater. Chem.* **2009**, *19*, 7362−7370.
(56) Wang, X.-S.; Ma, S.; Rauch, K.; Simmons, J. M.; Yuan, D.; Wang, X.; Yildirim, T.; Cole, W. C.; López, J. J.; Meijere, A. D.; et al. Metal−Organic Frameworks Based on Double-Bond-Coupled Di-isophthalate Linkers with High Hydrogen and Methane Uptakes. *Chem. Mater.* **2008**, *20*, 3145−3152.
(57) Llewellyn, P. L.; Bourrelly, S.; Serre, C.; Vimont, A.; Daturi, M.; Hamon, L.; Weireld, G. D.; Chang, J.-S.; Hong, D.-Y.; Hwang, Y. K.; et al. High Uptakes of CO_2 and CH_4 in Mesoporous Metal−Organic Frameworks MIL-100 and MIL-101. *Langmuir* **2008**, *24*, 7245−7250.
(58) Seki, K. Design of an Adsorbent with an Ideal Pore Structure for Methane Adsorption Using Metal Complexes. *Chem. Commun.* **2001**, 1496−1497.
(59) Senkovska, I.; Kaskel, S. High Pressure Methane Adsorption In The Metal−Organic Frameworks $Cu_3(btc)_2$, $Zn_2(bdc)_2$dabco, and $Cr_3F(H_2O)_2O(bdc)_3$. *Microporous Mesoporous Mater.* **2008**, *112*, 108−115.
(60) Wang, H.; Getzschmann, J.; Senkovska, I.; Kaskel, S. Structural Transformation And High Pressure Methane Adsorption Of Co_2(1,4-bdc)$_2$dabco. *Microporous Mesoporous Mater.* **2008**, *116*, 653−657.
(61) Getzschmann, J.; Senkovska, I.; Wallacher, D.; Tovar, M.; Fairen-Jimenez, D.; Düren, T.; Baten, J. M. v.; Krishna, R.; Kaskel, S. Methane Storage Mechanism In The Metal−Organic Framework $Cu_3(Btc)_2$: An in Situ Neutron Diffraction Study. *Microporous Mesoporous Mater.* **2010**, *136*, 50−58.
(62) García-Sánchez, A.; Dubbeldam, D.; Calero, S. Modeling Adsorption and Self-Diffusion of Methane in LTA Zeolites: The Influence of Framework Flexibility. *J. Phys. Chem. C* **2010**, *114*, 15068−15074.
(63) Awati, R. V.; Ravikovitch, P. I.; Sholl, D. S. Efficient and Accurate Methods for Characterizing Effects of Framework Flexibility on Molecular Diffusion in Zeolites: CH_4 Diffusion in Eight Member Ring Zeolites. *J. Phys. Chem. C* **2013**, *117*, 13462−13473.
(64) Kim, J.; Maiti, A.; Lin, L.-C.; Stolaroff, J. K.; Smit, B.; Aines, R. D. New Materials For Methane Capture From Dilute And Medium-Concentration Sources. *Nature Commun.* **2013**, *4*, 1694.
(65) Becke, A. D. Density-Functional Thermochemistry. III. The Role of Exact Exchange. *J. Chem. Phys.* **1993**, *98*, 5648−5652.
(66) Lee, C.; Yang, W.; Parr, R. G. Development of the Colle−Salvetti Correlation-Energy Formula into a Functional of the Electron Density. *Phys. Rev. B* **1988**, *37*, 785−789.
(67) Hehre, W. J.; Radom, L.; Schleyer, P. v. R.; Pople, J. A. *Ab Initio Molecular Orbital Theory*; Wiley: New York, 1988.

(68) Zhao, Y.; Truhlar, D. G. Density Functionals with Broad Applicability in Chemistry. *Acc. Chem. Res.* **2008**, *41*, 157−167.
(69) Tomasi, J.; Persico, M. Molecular Interactions in Solution: An Overview of Methods Based on Continuous Distributions of the Solvent. *Chem. Rev.* **1994**, *94*, 2027−2094.
(70) Cossi, M.; Barone, V.; Cammi, R.; Tomasi, J. Ab Initio Study of Solvated Molecules: A New Implementation of the Polarizable Continuum Model. *Chem. Phys. Lett.* **1996**, *255*, 327−335.
(71) Barone, V.; Cossi, M.; Tomasi, J. A New Definition Of Cavities for the Computation of Solvation Free Energies by the Polarizable Continuum Model. *J. Chem. Phys.* **1997**, *107*, 3210−3221.
(72) Barone, V.; Cossi, M.; Tomasi, J. Geometry Optimization of Molecular Structures in Solution by the Polarizable Continuum Model. *J. Comput. Chem.* **1998**, *19*, 404−417.
(73) Cossi, M.; Barone, V. Analytical Second Derivatives of the Free Energy in Solution by Polarizable Continuum Models. *J. Chem. Phys.* **1998**, *109*, 6246−6254.
(74) Camaioni, D. M.; Schwerdtfeger, C. A. Comment on "Accurate Experimental Values for the Free Energies of Hydration of H^+, OH^-, and H_3O^+. *J. Phys. Chem. A* **2005**, *109*, 10795−10797.
(75) Topol, I. A.; Tawa, G. J.; Burt, S. K.; Rashin, A. A. Calculation of Absolute and Relative Acidities of Substituted Imidazoles in Aqueous Solvent. *J. Phys. Chem. A* **1997**, *101*, 10075−10081.
(76) Magill, A. A.; Cavell, K. J.; Yates, B. F. Basicity of Nucleophilic Carbenes in Aqueous and Nonaqueous SolventsTheoretical Predictions. *J. Am. Chem. Soc.* **2004**, *126*, 8717−8724.
(77) Brown, T. N.; Mora-Diez, N. Computational Determination of Aqueous pK_a Values of Protonated Benzimidazoles. *J. Phys. Chem. B* **2006**, *110*, 9270−9279.
(78) Trummal, A.; Rummel, A.; Lippmaa, E.; Burk, P.; Koppel, I. A. IEF-PCM Calculations of Absolute pK_a for Substituted Phenols in Dimethyl Sulfoxide and Acetonitrile Solutions. *J. Phys. Chem. A* **2009**, *113*, 6206−6212.
(79) Politzer, P.; Murray, J. S. In *Reviews in Computational Chemistry*; Lipkowitz, K. B., Boyd, D. B., Eds.; VCH Publishers: New York, 1991; Vol. 2, Chapter 7, pp 273−312.
(80) Tomasi, J.; Bonaccorsi, R.; Cammi, R. *Theoretical Models of Chemical Bonding*; Springer: Berlin, 1990; pp 230−268.
(81) Pathak, R. K.; Gadre, S. R. Maximal and Minimal Characteristics of Molecular Electrostatic Potentials. *J. Chem. Phys.* **1990**, *93*, 1770−1773.
(82) Scrocco, E.; Tomasi, J. Electronic Molecular Structure, Reactivity and Intermolecular Forces: An Euristic Interpretation by Means of Electrostatic Molecular Potentials. *Adv. Quantum Chem.* **1979**, *11*, 115−193.
(83) Murray, J. S.; Politzer, P. Statistical Analysis of the Molecular Surface Electrostatic Potential: An Approach to Describing Noncovalent Interactions in Condensed Phases. *J. Mol. Struct.: THEOCHEM* **1998**, *425*, 107−114.
(84) Brinck, T.; Murray, J. S.; Politzer, P. Quantative Determination of the Total Local Polarity (Charge Separation) in Molecules. *Mol. Phys.* **1992**, *76*, 609−617.
(85) Murray, J. S.; Politzer, P. Electrostatic Potentials of Amine Nitrogens as a Measure of the Total Electron-Attracting Tendencies of Substituents. *Chem. Phys. Lett.* **1988**, *152*, 364−370.
(86) Haeberlein, M.; Murray, J. S.; Brinck, T.; Politzer, P. Calculated Electrostatic Potentials and Local Surface Ionization Energies of Para-Substituted Anilines As Measures Of Substituent Effects. *Can. J. Chem.* **1992**, *70*, 2209−2214.
(87) Suresh, C. H. A Molecular Electrostatic Potential Approach to Determine the Steric Effect of Phosphine Ligands in Organometallic Chemistry. *Inorg. Chem.* **2006**, *45*, 4982−4986.
(88) Frisch, M. J.; Trucks, G. W.; Schlegel, H. B.; Scuseria, G. E.; Robb, M. A.; Cheeseman, J. R. J.; Montgomery, A., Jr.; Vreven, T.; Kudin, K. N.; Burant, J. C.; et al. *Gaussian 03*, revision E.01; Gaussian, Inc.: Wallingford, CT, 2004.
(89) Frisch, M. J.; Trucks, G. W.; Schlegel, H. B.; Scuseria, G. E.; Robb, M. A.; Cheeseman, J. R.; Scalmani, G.; Barone, V.; Mennucci, B.; Petersson, G. A.; et al. *Gaussian 09*, revision B01; Gaussian, Inc: Wallingford, CT, 2010.
(90) Su, P.; Li, H. Energy Decomposition Analysis of Covalent Bonds and Intermolecular Interactions. *J. Chem. Phys.* **2009**, *131*, 014102.
(91) Schmidt, M. W.; Baldridge, K. K.; Boatz, J. A.; Elbert, S. T.; Gordon, M. S.; Jensen, J. H.; Koseki, S.; Matsunaga, N.; Nguyen, K. A.; Su, S.; et al. General Atomic and Molecular Electronic Structure System. *J. Comput. Chem.* **1993**, *14*, 1347−1363.
(92) Vijay, D.; Sakurai, H.; Subramanian, V.; Sastry, G. N. Where to Bind in Buckybowls? The Dilemma of a Metal Ion. *Phys. Chem. Chem. Phys.* **2012**, *14*, 3057−3065.
(93) Thellamurege, N.; Hirao, H. Water Complexes of Cytochrome P450: Insights from Energy Decomposition Analysis. *Molecules* **2013**, *18*, 6782−6791.
(94) Alder, R. W.; Bowman, P. S.; Steele, R. W. S.; Winterman, D. R. The Remarkable Basicity of 1,8-Bis(dimethylamino)naphthalene. *J. Chem. Soc., Chem. Commun.* **1968**, 723−724.
(95) Decouzon, M.; Gal, G. F.; Maria, P. C.; Raczynska, E. D. Superbases in the Gas Phase: Amidine and Guanidine Derivatives with Proton Affinities Larger than 1000 kJ mol^{-1}. *Rapid Commun. Mass Spectrom.* **1993**, *7*, 599−602.
(96) Despotović, I.; Maksić, Z. B.; Vianello, R. Design of Bronsted Neutral Organic Bases and Superbases by Computational DFT Methods: Cyclic and Polycyclic Quinones and [3]Carbonylradialenes. *Eur. J. Org. Chem.* **2007**, 3402.
(97) Tonner, R.; Heydenrych, G.; Frenking, G. First and Second Proton Affinities of Carbon Bases. *ChemPhysChem* **2008**, *9*, 1474−1481.
(98) Maksić, Z. B.; Vianello, R. Quest for the Origin of Basicity: Initial vs Final State Effect in Neutral Nitrogen Bases. *J. Phys. Chem. A* **2002**, *106*, 419−430.
(99) Kovačević, B.; Maksić, Z. B. Basicity of Some Organic Superbases in Acetonitrile. *Org. Lett.* **2001**, *3*, 1523−1526.
(100) Kaljurand, I.; Kütt, A.; Sooväli, L.; Rodima, T.; Mäemets, V.; Leito, I.; Koppel, I. A. Extension of the Self-Consistent Spectrophotometric Basicity Scale in Acetonitrile to a Full Span of 28 pK_a Units: Unification of Different Basicity Scales. *J. Org. Chem.* **2005**, *70*, 1019−1028.
(101) Liao, S.-M.; Du, Q.-S.; Meng, J. −Z.; Pang, Z.-W.; Huang, R.-B. The Multiple Roles of Histidine in Protein Interactions. *Chem. Cent. J.* **2013**, *7*, 44−56.
(102) Tukov, A. A.; Normand, A. T.; Nechaev, M. S. *N*-Heterocyclic carbenes bearings two, one and no nitrogen atoms at the ylidene carbon: insight from theoretical calculations. *Dalton Trans.* **2009**, 7015−7028.
(103) Pan, S.; Banerjee, S.; Chattaraj, P. K. Role of Lithium Decoration on Hydrogen Storage Potential. *J. Mex. Chem. Soc.* **2012**, *56*, 229−240.
(104) Srinivasu, K.; Ghosh, S. K.; Das, R.; Giri, S.; Chattaraj, P. K. Theoretical Investigation of Hydrogen Adsorption in All-Metal Aromatic Clusters. *RSC Advances* **2012**, *2*, 2914−2922.
(105) Lochan, R. C.; Head-Gordon, M. Computational Studies of Molecular Hydrogen Binding Affinities: The Role of Dispersion Forces, Electrostatics, and Orbital Interactions. *Phys. Chem. Chem. Phys.* **2006**, *8*, 1357−1370.
(106) Andreychuk, N. R.; Emslie, D. J. H. Potassium−Alkane Interactions within a Rigid Hydrophobic Pocket. *Angew. Chem., Int. Ed.* **2013**, *52*, 1696−1699.
(107) Parr, R. G.; Chattaraj, P. K. Principle of Maximum Hardness. *J. Am. Chem. Soc.* **1991**, *113*, 1854−1855.
(108) Chamorro, E.; Chattaraj, P. K.; Fuentealba, P. Variation of the Electrophilicity Index along the Reaction Path. *J. Phys. Chem.* **2003**, *107*, 7068−7072.